HEAT REMOVAL CAPACITY OF HEAT PIPE DESIGN FOR IN-CORE PASSIVE DECAY HEAT REMOVAL SYSTEM

Kyung Mo Kim, In Guk Kim, Yeong Shin Jeong, In Cheol Bang*
School of Mechanical and Nuclear Engineering
Ulsan National Institute of Science and Technology
50 UNIST-gil, Ulju-gun, Ulsan, 689-798, Republic of Korea
icbang@unist.ac.kr

ABSTRACT

A passive in-core cooling system (PINCs) can be adopted in control rods for passive safety of advanced nuclear power plants. A hybrid heat pipe is a heat transfer device to take the roles of both neutron absorption and heat removal by combining the functions of a heat pipe and a control rod. The unique characteristic of the hybrid control rod is the presence of neutron absorber inside the heat pipe. Many previous researchers studied the effect of parameters on the thermal performance of heat pipe. However, the effect of inner structure on the thermal performance of heat pipe has not been investigated. As a first step of the development of hybrid heat pipe, the annular heat pipe which contains neutron absorber in the normal heat pipe was prepared and the thermal performance of the annular heat pipe was experimentally studied. The annular heat pipe showed higher thermal resistances in the evaporator region with a maximum increase of 100 %, although condenser thermal resistances and total thermal resistances were was similar with those of normal heat pipe. In the aspect of operational limit, the annular heat pipe showed lower maximum heat transfer capacity than a normal heat pipe due to a smaller cross-section of vapor path in evaporator region, which resulted in high shear at the vapor-liquid interface of the wick structure. In addition, several further works to assess the effect of inner structure on the maximum heat removal rate of the hybrid heat pipe were presented.

KEYWORDS
Hybrid heat pipe, Passive IN-core Cooling system (PINCs), Annular heat pipe, Neutron absorber

1. INTRODUCTION

Development of advanced passive decay heat removal systems in nuclear power plants has been a hot issue due to severe accidents such as Fukushima and Three Mile Island (TMI) accidents. However, in case of most of passive decay heat removal systems, the main function is characterized by how to feed additional coolant to the reactor core according to accident scenarios. Especially, when station blackout (SBO) accident occurs, the established emergency core cooling systems cannot operate properly due to the difficulty of depressurization. Therefore, a new concept of passive decay heat removal system to mitigate the SBO accidents is required. In this research, an innovative hybrid control rod concept is considered for passive in-core decay heat removal. A heat pipe is a device that transfers heat from the hot interface to the cold one by phase change and capillary action of working fluid. The concept of the hybrid control rod is that the control rod can have not only the original function of neutron absorber but also the

* Corresponding author: Tel:+82-52-217-2915, Fax:+82-52-217-3008
E-mail : icbang@unist.ac.kr (In Cheol Bang)

function of the heat removal. In other words, if the function of a heat pipe is combined to the control rods, the limited heat removal capacity in an accident can be extended because control rods always are inserted to the reactor core at initial state of an accident using gravitational force. The hybrid control rod operates by temperature difference between the heat sink and active core of the reactor pressure vessel (RPV) as shown in Figure 1. The existing control rods are hold by spider grid which connected to the control rod drive mechanism (CRDM). However, the hybrid heat pipe must be extended from active core to the heat sink for the heat transport. Also, more passages which hybrid heat pipes can move along the axial direction at the upper head of RPV must be retained. The scheme of hybrid heat pipe is also introduced in Figure 1. The temperature difference between the upper plenum (assuming the upper plenum act as heat sink of the hybrid control rods) and active core is about 20 K at normal operating condition and initial condition of accident in the case of APR1400. And the maximum heat removal capacity of heat pipe is determined by capillary limit. The maximum heat removal capacity of the hybrid control rod in temperature difference of 20 K is about 1.6 kW. If all control rods in APR1400 (756 ea) perform the decay heat removal, the total decay heat removal by hybrid control rod is 1.2 MW. The heat removal rate is about 3 % of decay heat when the decay heat removal from the secondary system is ended by depletion of water in the steam generator at SBO accident. Thus, the enhancement of heat removal capacity of hybrid control rod system is required.

If the ultimate heat sink is retained with 50 ^{o}C water, the heat removal capacity of the hybrid heat pipe is 18 kW (65 kW/m^2) for a single rod. The heat removal rate can delay time to the core uncovery about 325 minutes compared to the established reactor performance. And the 2.5 times enhancement of heat removal capacity of hybrid control rod can prevent the boiling of primary coolant and cool the reactor.

A heat pipe has a variety of advantages such as high heat removal rate per unit volume, fully passive working principle, easy applicability, and so on [1]. Therefore, heat pipes have been used in various thermal engineering fields such as CPU, spaceship nuclear reactor, and Trans-Alaska Pipeline system. Heat pipe applications to nuclear power plants have been studied with various concepts. Table 1 presents previous studies on application of heat pipes to nuclear power plants. Dunkel et al. [2] devised the in-vessel and ex-vessel decay heat removal systems using heat pipes under loss of coolant accident (LOCA) condition. The in-vessel cooling system applied heat pipes to control rod channels and the ex-vessel cooling system installed heat pipes on the ex-vessel wall. Mochizuki et al. [3] suggested the spent fuel pool cooling system using heat pipes. They observed the applicability of the system in terms of economy and heat removal by predicting temperature change of spent fuel pool at various conditions. Sviridenko [4] suggested a passive decay heat removal system using heat pipes on WWER. Various system designs have been proposed in his work. Gou et al. [5] proposed the heat pipe as heat transfer device between reactor vessel and nuclear steam supply system for the purpose of simplification of system. And they showed that alkali metal heat pipes for the cooling of spaceship nuclear reactors had significant heat transfer capacity.

However, all previous works are limited to the introduction of the heat pipe-driven concepts and prediction of their system effects without real tests. Also, most previous studies on the heat pipe were limited on the measurement of effects of various parameters such as fill ratio of working fluid, inclination angle, types of working fluid on the thermal performance of heat pipes in terms of thermal resistance and heat transfer coefficient.

In the present study, the hybrid control rod which plays roles of both neutron absorber and decay heat removal is newly considered and studied in terms of feasibility. The maximum heat transfer capacity of general heat pipe can be calculated with known correlations and physical models. However, the hybrid control rod must contain neutron absorber inside the heat pipe. Thus, the maximum heat removal capacity and thermal performance of hybrid heat pipe must be measured. So, the effect of presence of the neutron absorber on the thermal performance and maximum heat transfer capacity was investigated experimentally.

Table 1. Heat pipe applications to nuclear power plants

Researchers	Key concepts
Dunkel [2]	In-vessel heat pipe and Ex-vessel heat pipe cooling at LOCA
Mochizuki et al. [3]	Heat pipe decay heat removal system for spent fuel pool
Siviridenko [4]	Heat pipe decay heat removal system for WWER
Gou et al. [5]	Heat pipe system for heat transfer between RPV and steam supply system
Hu et al. [6]	Lithium and Potassium heat pipe for cooling system of nuclear fission reactor on Moon
Poston et al. [7]	High temperature heat pipe for small nuclear fission reactor of spaceship
Hejzlar et al. [8]	Sodium heat pipe for heat dissipation from vessel to earth

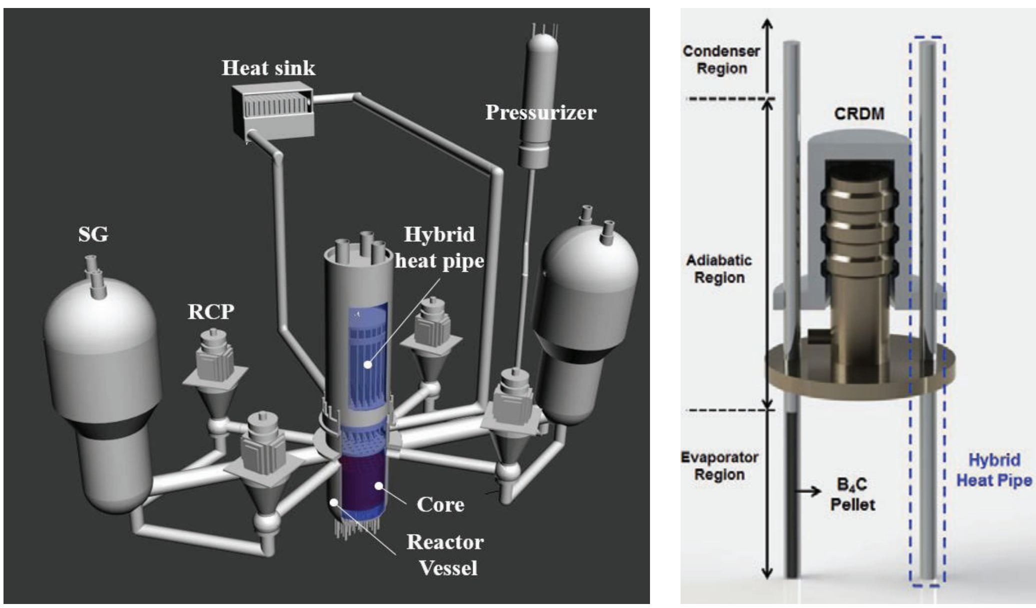

Figure 1. Systematic design of hybrid heat pipe as Passive IN-core Cooling system (PINCs) and hybrid heat pipe assembly

2. EXPERIMENTAL

2.1. Test section

The hybrid control rod is prepared based on information of established control rods in the commercial pressurized water reactor, APR-1400. Stainless steel 316L test sections having a sheath outer diameter of 1 in (25.4 mm outer diameter and 22 mm inner diameter) and length of 1000 mm were prepared with a single-layer screen wire mesh. The test section was charged with the working fluid at a 100% fill ratio (volume ratio of working fluid to wick structure).

B_4C pellet which is neutron absorber was then inserted in the center of heat pipe as shown in figure 2. The B_4C pellet has 17 mm outer diameter and 350 mm length. To prevent the effect of the pellet on the liquid flow through the test section, it was manufactured as non-porous structure.

Figure 2. Composition of hybrid control rod.

2.2. Experimental Setup and Procedure

Figure 3 shows the heat pipe test facility. The test facility comprises a working fluid tank, a test section, a water jacket to condense the evaporated working fluid, a pump that circulates coolant from the water storage tank to the water jacket, a vacuum pump, and two copper electrodes on the top and bottom of the evaporator section that are connected to the power supply and heat the test section by passing direct current.

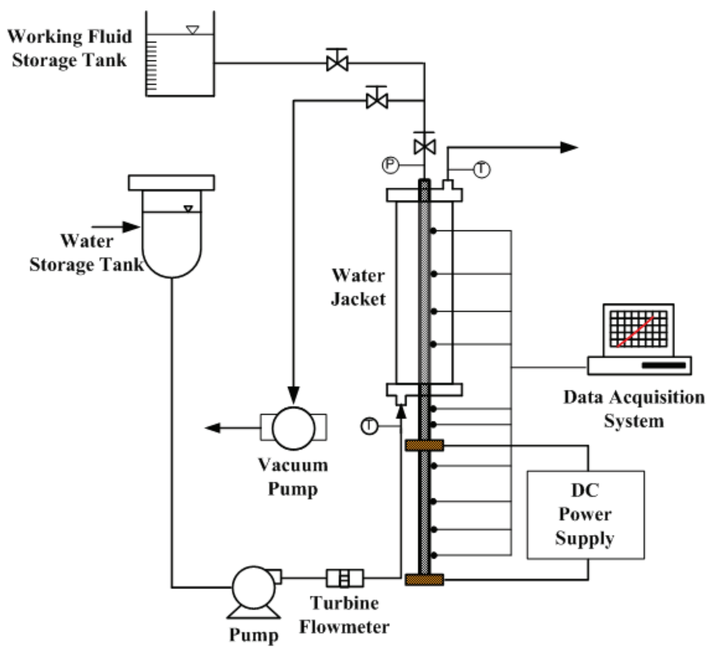

Figure 3. Schematic diagram of heat pipe test facility.

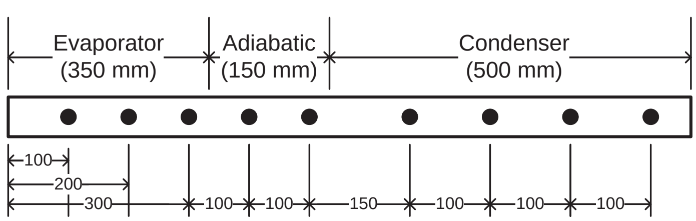

Figure 4. Thermocouple locations on the test section.

Figure 4 shows the thermocouple locations on the test section to measure the temperature distribution of the test section according to heat loads. Five K-type TCs were installed on the evaporator and adiabatic section of the test section (three for the evaporator and two for the adiabatic section), while four T-type TCs were installed on the condenser.

Table 2 present the experimental conditions. The experimental procedure is as follows. The pressure in the test section was set to 12.5 kPa to remove the non-condensable gas by using a vacuum pump. Although the coolant temperature in APR1400 is relatively high, adjustment of working fluid temperature of heat pipe to the reactor condition is difficult. Thus, for the precise comparison of the heat transfer characteristics of the heat pipe, the internal pressure was set to arbitrary pressure. The water was passed through the water jacket with a mass flow rate of 0.133 kg/s. Two T-type thermocouples at the inlet and outlet of the water jacket are used to measure the temperature change to obtain the heat removal rate. Then, the working fluid was charged to the test section with 100 % fill ratio (volume ratio of working fluid to wick structure). The test sections were heated step by step.

Table 2. Experimental conditions

Length ratio [%] (evaporator : adiabatic : condenser)	35 : 15 : 50
Heat input [W]	120 – 1120
Initial pressure [kPa]	12.5
Fill ratio [%]	100
Wick type	250-mesh SS 304 screen wire mesh
Porosity, ε	0.62
Permeability, K [m^2]	1.9×10^{-10}

The lengths of active core and control rod drive mechanism in APR1400 were considered to determine the length ratio of evaporator section and condenser section. Thus, the length ratio was fixed as 35:15:50 in percent.

2.3. Uncertainty analysis

The uncertainties in the parameter measurements were analyzed. Table 3 presents the uncertainties in the instruments. The uncertainty in the heat input (ΔQ/Q) was 0.31%. The measurement uncertainties in the heat flux, heat transfer coefficient, and thermal resistance were calculated as follows [9]:

Table 3. Instrument uncertainties

Parameters	Instruments	Uncertainties
Temperature	Thermocouple	1 ^{o}C
Pressure	Pressure gauge	0.4 %
Water flow rate	Turbine flowmeter	0.5 %
Voltage	Voltmeter	0.3 %
Current	Amperometry	0.08 %

$$\frac{\Delta q''}{q''}=\sqrt{\left(\frac{\Delta Q}{Q}\right)^2+\left(\frac{\Delta(\Delta t)}{\Delta t}\right)^2} \qquad (1)$$

$$\frac{\Delta h}{h}=\sqrt{\left(\frac{\Delta q''}{q''}\right)^2+\left(\frac{\Delta(\Delta T)}{\Delta T}\right)^2} \tag{2}$$

$$\frac{\Delta R}{R}=\sqrt{\left(\frac{\Delta Q}{Q}\right)^2+\left(\frac{\Delta(\Delta T)}{\Delta T}\right)^2} \tag{3}$$

The uncertainty in the area was neglected because the length and diameter of the test section were fixed at constant values. The calculated maximum uncertainties in the input heat flux and condensation heat flux were 5.5% and 3.75%, respectively. Therefore, the maximum uncertainties in the heat transfer coefficient and thermal resistance were estimated to be 6.8% and 5.5%, respectively.

3. RESULTS AND DISCUSSIONS

3.1. Steady state operations

The thermal performances of heat pipes were investigated by measuring the temperature distributions along the heat pipe for each heat load. The steady states were achieved with increasing the heat loads. Figure 5 shows the temperature histories of the test section according to heat loads. As shown in Fig. 5, temperatures in the evaporator section and adiabatic section oscillate within ±5 ^{o}C at low heat loads. After reaching 450 W of heat load for normal heat pipe (250 W for annular heat pipe), the heat pipes were activated and operated normally by showing the stable temperature changes. The temperatures at condenser sections maintained about 5 ^{o}C. However, the wall temperatures of the condenser section slightly increased as heat load increased because the vapor from evaporator section released heat.

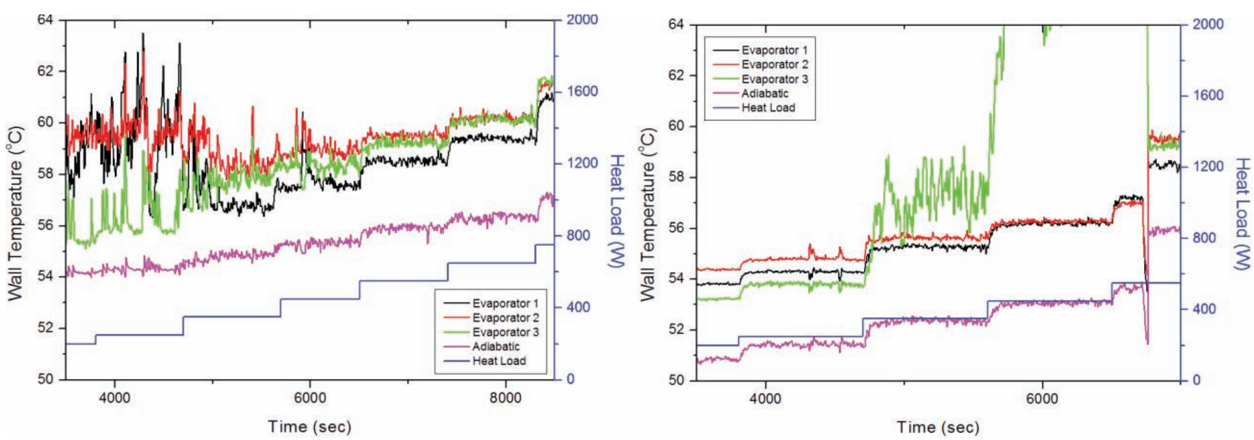

(a) Temperature histories of normal heat pipe (b) Temperature histories of annular heat pipe

Figure 5. Temperature histories of each test section according to heat loads

3.2. Temperature distributions

The steady states for each test section were achieved to measure the heat transfer characteristics of each section. Figure 6 show the temperature distributions of each test section according to heat loads at steady state condition.

As shown in Figure 6, the temperatures at the evaporator section increases as heat load increases. The temperatures at evaporator section of annular heat pipe were lower than those of normal heat pipe at same heat loads because the volume occupied by working fluid in the heat pipe is larger than normal heat pipe. At heat load of 450 W for the annular heat pipe, the sudden temperature increase was observed; while, the normal heat pipe showed general temperature distribution along the test section. The phenomenon indicates the operation limit of the test section. The operation limit of the annular heat pipe will be discussed in Section 3.5.

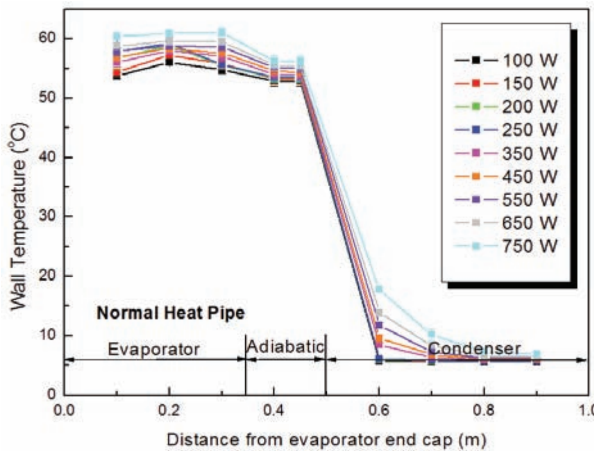

(a) Temperature distributions of normal heat pipe

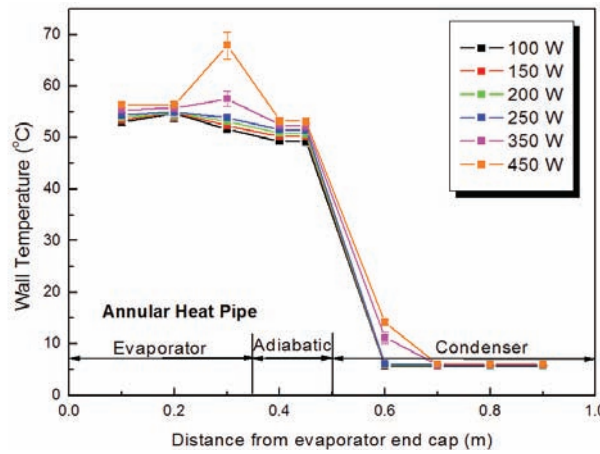

(b) Temperature distributions of annular heat pipe

Figure 6. Temperature distributions of each test section according to heat loads

3.3. Saturation temperatures

The internal pressures of the test sections were measured according to heat loads to observe the saturation temperatures. Although some previous studies [10 – 13] assumed the temperature in the adiabatic section as saturation temperature, axial heat conduction could affect to the temperature in the adiabatic section. Thus, the internal pressures were measured. The saturation temperatures observed by internal pressures were compared with temperature at the adiabatic section. The differences between saturation temperature calculated by internal pressure and adiabatic section temperature are within 1 ^{o}C. Thus, the thermal resistances of the test sections were calculated with the saturation temperature observed by measured internal pressures.

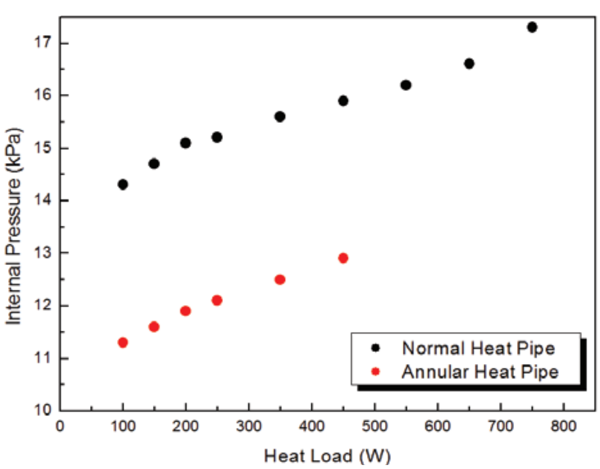

(a) Internal pressures of each test section

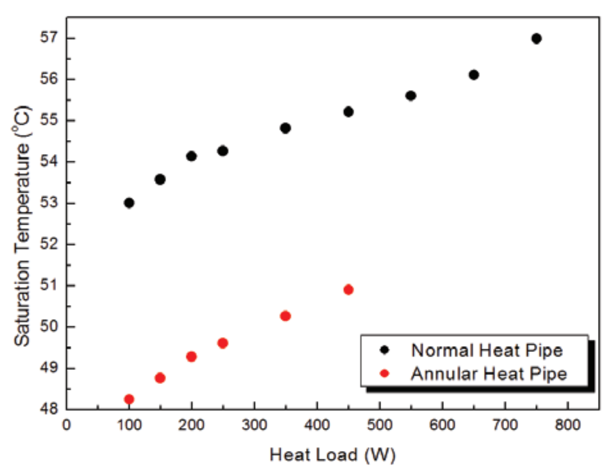

(b) Saturation temperatures of each test section

Figure 7. Internal pressures and saturation temperatures of each test section according to heat loads

3.4. Thermal resistances

The evaporation, condensation, and overall thermal resistances (R_e, R_c, and R_{tot}) were calculated by the below equations:

$$R_e = \frac{\left(\bar{T}_e - T_{sat}\right)}{Q_e} \qquad (4)$$

$$R_c = \frac{\left(T_{sat} - \bar{T}_c\right)}{Q_c} \qquad (5)$$

$$R_{tot} = \frac{\left(\bar{T}_e - \bar{T}_c\right)}{Q_e} \qquad (6)$$

Thermal resistances of each test section were measured using the temperature distribution and saturation temperature. The saturation temperature was measured by recording internal pressure of the test section and the saturation temperature was validated with temperature of the adiabatic section.

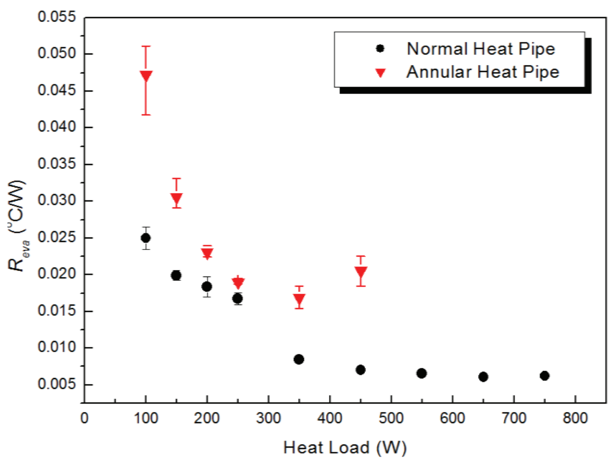

(a) Evaporator thermal resistance of each test section

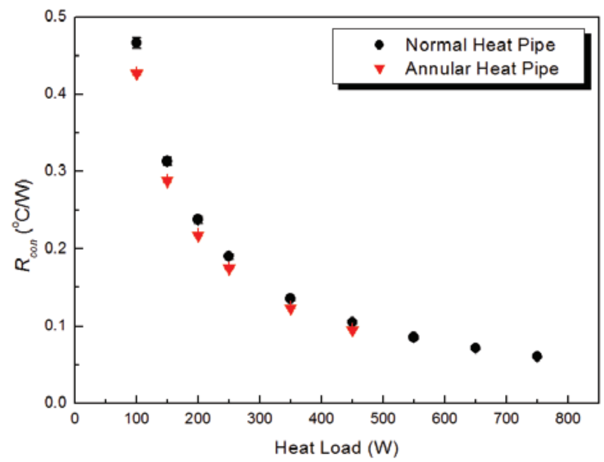

(b) Condenser thermal resistances of each test section

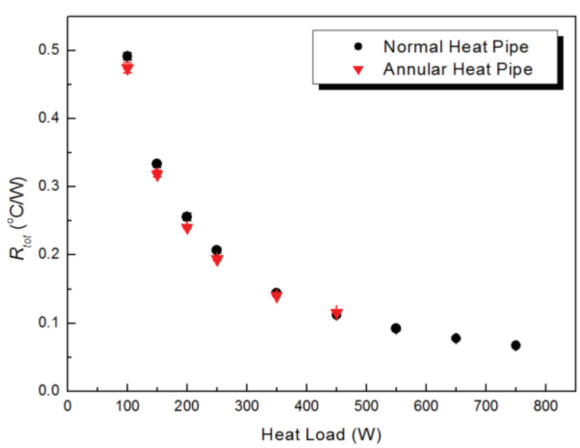

(c) Total thermal resistances of each test section

Figure 8. Thermal resistances of each test section according to heat loads

As shown in Figure 8(a), the annular heat pipe shows higher evaporator thermal resistances because the larger volume of working fluid formed thicker liquid layer at the inner wall of test section.

The level of working fluid is located in the adiabatic section in the case of annular heat pipe. Thus, the evaporation of working fluid will be suppressed. This phenomena reduces the amount of evaporized vapor, finally, the liquid sublayer at condenser section will be decreased. As a result, the condenser thermal resistances of annular heat pipe were lower than those of normal heat pipe as shown in Figure 8(b). The liquid thickness at the condenser section is thicker than the evaporator section. So, the condenser thermal resistances are higher than evaporator thermal resistances for each test section and the thermal resistances at the condenser section dominate the total resistance of heat pipe. Hence, the annular heat pipe shows higher total thermal resistances than normal heat pipe as shown in Figure 8(c).

3.5. Operational limits

In order to remove large amount of the decay heat from the reactor core at accident conditions, the maximum heat removal capacity must be ensured. The heat pipes have five types of operational limits; viscous limit, sonic limit, entrainment limit, boiling limit, and capillary limit. Generally, the capillary limit is the main concern to consider as the lowest operational limit, which is caused by a limitation of liquid flow through the wick structure against pressure losses inside the heat pipe. When the heat load reaches the capillary limit, the temperature of the evaporator section will be increased.

The capillary limit occurs when the capillary pumping pressure becomes lower than pressure losses as expressed as equation [14]:

$$\frac{2\sigma}{r_{ce}} < \left(\frac{Cf_v \operatorname{Re}_v \mu_v}{2r_{hv}^2 A_v \rho_v \lambda} L_{eff} Q \right) + \left(\frac{\mu_l}{KA_w \rho_l \lambda} L_{eff} Q \right) + \left(\rho_l g d_v \cos\psi \right) + \left(\rho_v g L_{eff} \sin\psi \right) \quad (7)$$

The left hand side term is the capillary pumping pressure and the right hand side terms are viscous pressure losses in vapor, inertial and viscous pressure losses in liquid, normal hydrostatic pressure losses, and axial hydrostatic pressure losses in order. The capillary pumping pressure and other pressure losses are the same with the normal heat pipe, except the viscous pressure losses in vapor in the annular heat pipe that contains B_4C pellets. The presence of inner structure (B_4C pellet) decreases the hydraulic radius of the vapor space (r_{hv}) and area of the vapor space (A_v) increasing the friction factor (f_v) and Reynolds number (Re_v) in the condition of same vapor volume flow rate. Therefore, the viscous pressure losses in vapor would increase, which results in the capillary limit of the annular heat pipe to be lower than that of a normal heat pipe.

Figure 6 shows the temperature increase at the top of evaporator section at 450 W and the liquid level is enough to fill the gap between the B_4C pellet and inner wall of the heat pipe. Thus, this phenomenon can be interpreted as the capillary limit.

After reaching the capillary limit, the evaporator thermal resistance was increased as shown in Figure 5. However, the limitation was not observed in the normal heat pipe with the same heat load. The neutron absorber (B_4C pellet) reduced the cross section of vapor flow path resulting in higher vapor velocity. As a result, viscous pressure loss in vapor increased and the maximum heat removal capacity was observed to be lower, compared to the normal heat pipe.

3.6. Further works

The operational limit (450 W, 18.6 kW/m^2) of the annular heat pipe containing the neutron absorber (B_4C pellet of 17 mm diameter and 350 mm length) corresponds to 1/3.5 of the heat flux of the hybrid heat pipe (65 kW/m^2), when the temperatures of primary coolant and ultimate heat sink are 320 ^{o}C and 50 ^{o}C. So, 8.5 times of enhancement of operation limit of the annular heat pipe is required in terms of heat flux to prevent the boiling of primary coolant and core uncovery. To increase the operational limit of the hybrid heat pipe, the high shear at the interface of vapor flow and liquid flow must be reduced. The present diameter of neutron absorber is 17 mm occupying a large portion of vapor flow path of the heat pipe. However, the reduction of the B_4C pellet diameter by enrichment of ^{10}B, which is the main isotope of neutron absorbing boron, can reduce the shear maintaining the reactivity control ability of the control rods. So, the effect of pellet diameter on the maximum heat removal capacity of the hybrid heat pipe will be studied.

The modified geometry of B_4C pellets which have the same neutron absorption cross-sectional area and the expanded vapor flow path also can be designed. Additional design candidates of the hybrid heat pipe can enhance the maximum heat removal rate.

The main restrictions of the heat transfer through the heat pipe are the capillary limit and the boiling limit. Thus, the liquid flow rate through the wick structure and liquid supply on the inner wall of the evaporator section are the key phenomena in terms of capillary limit and boiling limit. Nanofluids and surface modification technology are under study as a means to enhance boiling crisis from the view point of capillary pumping, roughness, wettability, and so on. Thus, the studies on the enhancement of boiling limit and capillary limit will be conducted using various nanofluids and modified surfaces.

4. CONCLUSIONS

A hybrid control rod concept was developed as a passive safety system of nuclear power plant to ensure the safety of the reactor during accident conditions. The hybrid control rod must contain the neutron absorber for the function as a control rod. So, the effect of neutron absorber on the thermal performance of heat pipe was experimentally investigated in this study. The following are the key observations:

(1) Temperature distributions at the evaporator section of annular heat pipe were lower than normal heat pipe due to the larger volume occupied by working fluid at the evaporator section.
(2) The evaporator thermal resistance of annular heat pipe was higher than normal heat pipe due to suppressed evaporation of working fluid at the same filling ratio of working fluid
(3) Annular heat pipe showed similar condenser and total thermal resistances with those of normal heat pipe due to almost same liquid thickness at the condenser section.
(4) The maximum heat removal capacity of annular heat pipe was lower than normal heat pipe because the reduced vapor flow path resulted in larger shear force at the vapor-liquid interface.
(5) Studies on enhancement of maximum heat removal capacity of the hybrid heat pipe will be studied modifying the design of hybrid heat pipe and using technologies associated with the enhancement of boiling crisis.

NOMENCLATURE

A	Area	[m^2]
C	Correlation coefficient	
f	friction factor	
g	gravity	
K	permeability	[m^2]
L	length	[m]
M	number of wires per inch	
Q	heat input, power	[W]
q''	heat flux	[kW/m^2]
r	radius	[m]
R	thermal resistance	[°C/W]
Re	Reynolds number	
t	temperature difference between evaporator section and condenser section	[°C]
T	temperature	[°C]

Greek symbols

ε	porosity	
ρ	density	[kg/m^3]
σ	surface tension	[N/m]
μ	dynamic viscosity	[Pa·s]
λ	latent heat of vaporization	[kJ/kg]
ψ	tilt angle	

Subscript

c	condenser
ce	effective capillary
e	evaporator
eff	effective
h	hydraulic
l	liquid
sat	saturation
tot	total
v	vapor
w	wick

ACKNOWLEDGMENTS

This work was supported by the Nuclear Energy Research Program through the National Research Foundation of Korea (NRF) funded by the Ministry of Science, ICT, and Future Planning. (No. 2013M2A8A1041442)

REFERENCES

1. D. A. Reay, P. A. Kew, Heat Pipes (fifth edition), Butterworth-Heinemann, Oxford (2006)
2. T. L. Dunkel, “Emergency heat removal system for a nuclear reactor”, United States Patent (1976)
3. M. Mochizuki, T. Nguyen, K. Mashiko, Y. Saito, R. Singh, T. Nguyen, V. Wuttijumnong, "Prevention possibility of nuclear power reactor meltdown by use of heat pipes for passive cooling of spent fuel", Frontiers in Heat Pipes (2013)
4. I. I. Sviridenko, "Heat exchangers based on low temperature heat pipes for autonomous emergency WWER cooldown systems", Applied Thermal Engineering, **28**, pp. 327-334 (2008)
5. P. F. Gou, Saratoga, L. E. Fennern, S. Jose, C. D. Sawyer, L. Gatos, "Nuclear reactor heat pipe", United States Patent (1997)
6. G. Hu, S. Zhao, Z. Sun, C. Yao, "A heat pipe cooled modular reactor concept for manned lunar base application", Proceedings of 2013 21st International Conference on Nuclear Engineering, **2** (2013)
7. D. Poston, R. Kapernick, D. Dixon, E. Reid, L. Mason, "Reactor module design for a killowatt-class space reactor power system", Nuclear and Emerging Technologies for Space (2012)
8. P. Hejzlar, N. E. Todreas, M. J. Driscoll, "Passive decay heat removal in advanced LWR concepts", Nuclear Engineering and Design, **139**, pp. 59-81 (1993)
9. A. B. Solomon, K. Ramachandran, B. C. Pillai, "Thermal performance of a heat pipe with nanoparticles coated wick", Applied Thermal Engineering, **36**, pp. 106-112 (2012).
10. P. Y. Wang, X. J. Chen, Z. H. Liu, Y. P. Liu, "Application of nanofluid in an inclined mesh wicked heat pipes", Thermochimica Acta, **539**, pp. 100-108 (2012)
11. W. N. Septiadi, N. Putra, M. Juarsa, I. P. A. Putra, R. Sahmura, "Characteristics of screen mesh wick heat pipe with nanofluid as passive cooling system", Atom Indonesia, **39**, pp. 24-31 (2013).
12. N. Putra, W. N. septiadi, H. Rahman, R. Irwansyah, "Thermal performance of screen mesh wick heat pipes with nanofluids", Experimental Thermal and Fluid Science, **40**, pp. 10-17 (2012)
13. K. H. Do, H. J. Ha, S. P. Jang, "Thermal resistance of screen wire mesh heat pipes using the water-based Al_2O_3 nanofluids", International Journal of Heat and Mass Transfer, **53**, pp. 5888-5894 (2010).
14. G. P. Peterson, *An introduction to heat pipe; Modeling, testing and applications*, John Wiey & Sons., New York, NY, USA (1994)